HHS Public Access

Author manuscript

Sci Transl Med. Author manuscript; available in PMC 2017 May 31.

Published in final edited form as:

Sci Transl Med. 2014 September 03; 6(252): 252ra124. doi:10.1126/scitranslmed.3009443.

The HMGB1-RAGE Axis Mediates Traumatic Brain Injury-induced Pulmonary Dysfunction in Lung Transplantation

Daniel J. Weber[1,2], **Adam S.A. Gracon**[1,2], **Matthew S. Ripsch**[3], **Amanda J. Fisher**[1,3], **Bo M. Cheon**[3], **Pankita H. Pandya**[1,4], **Ragini Vittal**[1,4], **Maegan L. Capitano**[4], **Youngsong Kim**[3], **Yohance M. Allete**[3], **Amanda A. Riley**[5], **Brian P. McCarthy**[5], **Paul R. Territo**[5], **Gary D. Hutchins**[5], **Hal E. Broxmeyer**[4], **George E. Sandusky**[6], **Fletcher A. White**[1,3,*], and **David S. Wilkes**[1,4,*]

[1]Center for Immunobiology, Indiana University School of Medicine, Indianapolis, IN

[2]Department of Surgery, Indiana University School of Medicine, Indianapolis, IN

[3]Department of Anesthesia, Paul and Carole Stark Neurosciences Research Institute, Indianapolis, IN

[4]Department of Microbiology and Immunology, Indiana University School of Medicine, Indianapolis, IN

[5]Department of Radiology and Imaging Sciences, Indiana University School of Medicine, Indianapolis, IN

[6]Department of Pathology, Indiana University School of Medicine, Indianapolis, IN

Abstract

Corresponding author: David S. Wilkes, MD, Indiana University School of Medicine, Fairbanks Hall, Suite 6200, Indianapolis, IN 46202, Telephone: (317) 278-7020, Fax: (317) 274-8349, dwilkes@iupui.edu.

*Dr. White and Dr. Wilkes are the senior co-authors for this manuscript.

Author contributions: Conception and design: DJW, FAW, DSW;
Analysis and Interpretation: DJW, ASG, MLC, PRT, GDH, HEB, GES, FAW, DSW;
Drafting the manuscript for important intellectual content: DJW, ASG, PRT, FAW, DSW
Animal studies and laboratory experiments:

Histology and Acute Lung Injury Scoring: DJW, GES

Traumatic Brain Injury Experiments: DJW, ASG, MSR

Murine Pulmonary Function Testing: DJW, AJF

Murine Lung Transplant Model: DJW, ASG

Cardiac Output Analysis: AAR, BPM, PRT

Cell Culture and Immunohistochemistry: PHP, RV, MLC, YMA, YK

Protein Analysis: BMC, YK, MLC

In Vivo Decoy Peptide Testing: YMA, MSR, DJW

Clinical Samples and Analysis: DJW

Competing interests: DW is a co-founder and chief scientific officer of ImmuneWorks, a biotech company developing therapeutics for immune-mediated lung diseases. The other authors declare that they have no competing interests.

Traumatic brain injury (TBI) results in systemic inflammatory responses that affect the lung. This is especially critical in the setting of lung transplantation where more than half of donor allografts are obtained postmortem from individuals with TBI. The mechanism by which TBI causes pulmonary dysfunction remains unclear but may involve the interaction of high mobility group box 1 (HMGB1) protein with the receptor for advanced glycation end products (RAGE). To investigate the role of HMGB1 and RAGE in TBI-induced lung dysfunction, RAGE sufficient (wildtype) or deficient (RAGE−/−) C57BL/6 mice were subjected to TBI through controlled cortical impact and studied for cardio-pulmonary injury. Compared to control animals, TBI induced systemic hypoxia, acute lung injury, pulmonary neutrophilia and decreased compliance, all of which were attenuated in RAGE −/− mice. Neutralizing systemic HMGB1, induced by TBI, reversed hypoxia and improved lung compliance. Compared to wildtype donors, lungs from RAGE−/− TBI donors did not develop acute lung injury after transplantation. In a study of clinical transplantation, elevated systemic HMGB1 in donors correlated with impaired systemic oxygenation of the donor lung pre-transplantation and predicted impaired oxygenation post-transplantation. These data suggest that the HMGB1-RAGE axis plays a role in the mechanism by which TBI induces lung dysfunction and that targeting this pathway prior to transplant may improve recipient outcomes following lung transplantation.

Introduction

In addition to the lesions caused at the moment of injury, brain trauma can result in secondary damage, which includes a variety of events that take place in the subsequent hours and days after injury. Included in the possible secondary injury types are indirect effects on the pulmonary system including acute respiratory distress syndrome (ARDS) and acute lung injury (ALI). This is particularly relevant in the context of lung transplantation where the majority of donor lungs are procured from brain-dead donors, of which between 40–70% have sustained traumatic brain injury (TBI) (1). Of those evaluated only approximately 15% are deemed suitable for transplant (2). The mechanisms by which TBI leads to pulmonary dysfunction are poorly understood. Historically, a combination of catecholamine surge-induced pulmonary vascular permeability, as well as production of inflammatory mediators are thought to compromise lung function (3). There is evidence that systemic inflammatory factors cause pulmonary injury and dysfunction (4).

Recent approaches to identifying the pathophysiological mechanisms of acute lung injury have focused on non-traditional pro-inflammatory mediators and their receptors. In particular is the class of danger-associated molecular patterns (DAMPs; alarmins), which are often associated with sterile inflammatory responses to events such as ischemia or systemic disease. A DAMP of particular interest is high mobility group box-1 (HMGB1). Though HMGB1 is typically associated with chromatin, it can be quickly released into the cytoplasm following stress, injury, or disease. Depending on the status of the affected cells, cytoplasmic HMGB1 can be passively released into the extracellular space. Alternatively, HMGB1 can be actively released by cells of the immune and nervous systems following injury, inflammation, or disease (5–7). Progress to date suggests that HMGB1 receptors include toll-like receptor 4 (TLR4) and receptor for advanced glycation end products (RAGE) (8). Both TLR4 and RAGE are expressed by many cell types including those in the lung (12) and

participate in the onset of innate immune inflammatory processes through activation of NF-κB (13, 14). HMGB1 binding to RAGE has also been implicated in a number of inflammation-associated diseases including cancer, diabetes, epilepsy, and Alzheimer's disease (9–11). It is well established that RAGE is constitutively expressed at high levels in the lung (12), and RAGE ligation leads to sustained activation of NF-κB and increased RAGE expression, which ensure maintenance and amplification of an inflammatory signal (13, 14).

In this study, we examined the involvement of HMGB1 and RAGE in TBI-induced acute lung injury in mice whose lungs were utilized as donors for transplantation. We also used clinical samples to explore the connection between elevated donor HMGB1 and pulmonary dysfunction before and after lung transplantation. As HMGB1 is known for its contribution to proinflammatory processes associated with injury and organ damage associated with severe sepsis, TBI disruption of the blood-brain barrier and the release of DAMPs could trigger an inflammatory cascade in tissues rich in RAGE receptors, most prominently the lungs (15–18). In an effort to characterize the cause of pulmonary dysfunction after TBI and the role of the HMGB1-RAGE axis, we studied lungs obtained from mice either deficient or sufficient in RAGE prior to being utilized as donors for transplantation. Local and systemic inflammatory responses as well as pulmonary function in both donors and recipients were analyzed. Translational studies examined the correlation of systemic HMGB1 concentrations and indices of acute lung injury in human lung transplant donors before donor harvest and in recipients after lung transplantation. Our objective was to determine whether TBI-induced inflammatory changes result in pulmonary dysfunction that is dependent on the HMGB1-RAGE pathway.

Results

TBI Induces Acute Lung Injury and Increased Systemic HMGB1

TBI caused substantial changes in lung architecture of C57BL/6 mice. These animals had evidence of alveolar hemorrhage at 4 and 8 hours post injury compared with sham-injured mice. By the 12 and 24 hour time points, this alveolar hemorrhage largely had resolved (Fig. 1A–E). However, these lungs did continue to have evidence of acute lung injury as evidenced by proteinaceous debris and neutrophilic infiltration. As scored by a standardized assessment (19), lungs from animals subjected to TBI had higher acute lung injury scores than control lungs at the same time intervals (Fig. 1F). The mean score for sham-injury control lungs was 0.09 ±0.03 while scores at the 4 hour time point after TBI yielded a significantly higher score of 0.62 ±0.11 ($p < 0.01$). Scores remained significantly elevated at 8, 12, and 24 hours after TBI with scores of 0.47 ±0.11, 0.49 ±0.16, and 0.56 ±0.15, respectively (all $p < 0.01$). Additionally, the amount of alveolar hemorrhage at the 4 and 8 hour time points corresponded with acute lung injury scores.

Consistent with neutrophilia in the lung were data showing that myeloperoxidase (MPO), a neutrophil-derived enzyme, was greater in mice subjected to TBI compared to controls (327 ±14.7 vs. 161 ±12.7 ng/mL, respectively, $p<0.01$, Fig. S1). Activated caspase-3 staining, a marker for apoptosis that can occur during tissue injury of many types including the lung,

was not increased in either C57BL/6 or RAGE−/− TBI mice compared to sham TBI mice (Fig. S2).

Albumin was quantitated in bronchalveolar lavage fluid (BAL) after TBI to determine if increased vascular permeability was associated with the acute lung injury scores. In healthy mice subjected to sham injury, the BAL albumin concentration was 52.5 ± 11.2 μg/mL. Albumin concentrations were significantly higher at 4 hours post TBI (303 ± 21.0 μg/mL) then declined progressively at 8 (301 ± 34.1 μg/mL), 12 (212 ± 17.9 μg/mL), and 24(103 ± 22.1 μg/mL) hours (Fig. 1G). However, compared to controls, all BAL albumin levels were increased significantly at each time point indicating TBI-induced vascular permeability ($p < 0.01$).

To determine if HMGB1 increased following TBI, serum HMGB1 levels from sham-injured wildtype mice as well as TBI wildtype mice were assayed at 24 hours (Fig. 1H). In sham-injury control animals, the mean serum HMGB1 concentration was 1.8 ± 0.4 ng/mL. However, TBI-induced significantly higher HMGB1 levels compared to controls (4.1 ±0.7 ng/mL, $p < 0.01$). Even higher levels were seen with RAGE −/− mice (7.9 ± 2.6 ng/ml, $p < 0.01$).

RAGE and HMGB1 Profiling

In an effort to confirm that RAGE, a key receptor for HMGB1, is organ specific, Western blots were performed using homogenates of lung, spleen, liver, and spinal cord from three wildtype mice. High levels of RAGE were present in the lung samples but not the other tissue types (Fig. S3). To localize possible serum sources of HMGB1, we profiled HMGB1 in both the lungs and cortical tissue ipsilateral to the TBI in sham and TBI mice. Although nuclear HMGB1 was observed in the lungs of both sham and TBI mice, there was no evidence of the loss of nuclear HMGB1 immunopositive signal (Fig. S4). In contrast, cortical tissue associated with the lesion site exhibited a pronounced decrease in the number of cells which were immunoreactive for HMGB1 when compared with adjacent, uninjured cortical areas 24 hours after TBI. The observed loss of cellular HMGB1in injured tissue did not appear to be associated with TBI-induced cell loss as numerous cells within the lesion site retained nuclear staining with DAPI (Fig. S5).

TBI Induces Pulmonary Dysfunction

Groups of wildtype C57BL/6 mice were subjected to severe TBI injury followed by assessment of systemic oxygenation as determined by PaO2/FiO2 ratios 4 – 24h post TBI (Fig 2A). This ratio divides the aterial oxygentation concerntation by the fraction of inspired oxygen where increasing values reflect improved ability of the lung to absorb oxygen from air. The sham-injury control group, PaO2/FiO2 ratios were normal at 578 ± 5.23. However, 4 hours after TBI the PaO2/FiO2ratio decreased to 351 ±2.55 and continued to decline at 24 hours (111.5 ±13.09). Pulmonary function testing at the same intervals demonstrated a similar time-dependent decline in compliance (measure of the lungs ability to expand) (Fig. 2B). For the sham-injury control group, compliance was 0.0315 ±0.0004 mL/cmH_2O. By eight hours after TBI, compliance decreased to 0.0286 ±0.0008 ($p = 0.01$) mL/cmH_2O and continued to decline for up to 24 hours. Compliance at 24 hours was 0.0205 ±0.0006

mL/cmH_2O, which was significantly lower than the control group ($p < 0.01$). Airway resistant values were also recorded but did not differ between the groups (Fig. S6).

Pulmonary Dysfunction due to TBI is diminished in the lungs of RAGE−/− mice

In a separate group of experiments, we determined the role of RAGE in TBI-induced lung dysfunction. Wildtype C57BL/6 and RAGE −/− mice were subjected to moderate or severe TBI and PaO2/FiO2ratios were assessed at 24 hours. The moderate and severely injured wildtype C57BL/6 mice exhibited low PaO2/FiO2values at 358 ±14 and 221 ±14, respectively. These values were significantly lower than the sham-injury control mice (554 ± 9.25) ($p<0.01$) (Fig. 2C). In contrast, RAGE −/− mice subjected to moderate TBI exhibited PaO2/FiO2ratios that registered at 541± 8.06 and did not differ from sham-injury PaO2/FiO2ratio values ($p = 0.32$). Similarly, RAGE −/− mice with severe TBI did not appear to be compromised by the injury with a PaO2/FiO2ratio of 447 ± 3.4, which was significantly higher than for the wildtype C57BL/6 mice subjected to the same severe TBI ($p<0.01$). Static compliance was also assessed in wildtype C57BL/6 and RAGE −/− mice subjected to moderate and severe TBI. Static compliance in sham control animals was 0.034 ±0.0003 mL/cmH_2O, whereas compliance declined 24 hours after moderate or severe TBI to 0.0302 ±0.0006 mL/cmH_2O or 0.0226 ±0.0009 mL/cmH_2O, respectively ($p<0.01$). Compliance values were improved significantly in RAGE −/− mice subjected to severe injury with a mean value of 0.0317 ±0.0006 mL/cmH_2O compared to the wildtype group subjected to the same injury ($p<0.01$) (Fig. 2D). Such results indicate that RAGE plays a major role in the pulmonary dysfunction seen in wildtype mice.

TBI causes Lung Dysfunction in TLR4 −/− Mice

In an effort to determine the degree to which TLR4, a key HMGB1 receptor, may contribute to lung dysfunction, we subjected TLR4 −/− mice to severe TBI and performed functional analyses after 24 hours. All studies were repeated with groups of mice separate from those reported in figures 1 and 2. The values from TLR4 −/− mice were compared with a new set of RAGE −/− mice subject to the same brain injury. The mean PaO2/FiO2ratio in the TLR4 −/− mice was 355 ±28 which was significantly lower than values present in control wildtype mice and RAGE −/− TBI mice ($p < 0.01$, Fig. 3A). Additionally, the static compliance value in the TLR4 −/− mice was 0.0220 ±0.0040 mL/cmH_2O, again significantly lower than the control and RAGE −/− mice groups ($p < 0.01$, Fig. 3B).

Effect of Neutralizing HMGB1 on Lung Dysfunction

To determine if HMGB1 is the primary ligand activating RAGE or TLR4 following TBI, wildtype C57BL/6 mice were treated with a HMGB1 neutralizing antibody (HMGB1 Ab) or control antibody prior to TBI. HMBG1 Ab treatment resulted in a PaO2/FiO2ratio of 408 ±15.6 at 24 hours after TBI (Fig. 3A) with a mean compliance of 0.0272 ±0.0015 (Fig. 3B). These values with the neutralizing antibody were significantly improved compared to values observed with the control antibody or in wildtype mice post TBI ($p < 0.01$). However, these values were not different from those observed in TLR4 −/− mice (Fig. 3A,B).

Preservation of Lung Function using a Toll/IL-1 receptor domain-derived decoy peptide

Toll-like receptors utilize common Toll-/Interleukin-1R Resistance domains (TIR), which are pivotal to both interactions of signaling proteins and signal transduction (20). As TLR TIR dimers serve as recruitment centers for TLR adapter proteins, it is possible to inhibit cellular signaling downstream of TLR4 using cell permeable decoy peptides as competitive inhibitors of protein-protein interactions (21). TIRAP and MyD88, known adaptor proteins for Toll-like receptor-4, also bind to phosphorylated RAGE (22, 23). Using the cell-permeating decoy peptide, TAT-4BB, to inhibit surface exposed segments of these adapter proteins, we targeted the ability of HMGB1 to produce signaling *in vivo* via either TLR4 or RAGE (24). Wildtype C57BL/6 mice were administered a TAT-4BB decoy peptide before exposure to severe TBI. The mean PaO2/FiO2ratio in these animals was 487.8 ±31.14 at 24 hours post injury, which was significantly higher than values derived from the TLR4 −/− TBI mice ($p=0.01$) but did not differ from RAGE −/− mice ($p=0.22$, Fig. 3A). Additionally, the static compliance value in the decoy peptide 4BB-treated mice was 0.0286 ±0.0050 mL/cmH_2O, which did not differ from TLR4 −/− ($p =0.33$) or RAGE −/− mice ($p = 0.55$, Fig. 3B).

TBI induces pulmonary dysfunction in the setting of preserved cardiac output

In an effort to ensure that TBI-induced pulmonary dysfunction was non-cardiogenic in nature, we utilized gated PET scans to calculate cardiac outputs from four sham-injury control mice and four mice 24 hours after severe brain injury (Fig. S7A). The data showed that there was no significant difference in heart rates between control animals (440.4 ±32.3 bpm) and TBI mice (441.7 ±18.8 bpm) (Fig. S7B). TBI mice did exhibit elevations in average stroke volumes (0.0436 ± 0.0026 mL) when compared with sham-injury control volumes (0.034± 0.0017 mL) (Fig. S7C). Despite the elevated stroke volumes in the sham-injury group, there was not a significant difference in cardiac output between the groups.

Murine lung transplant recipients from TBI donors exhibit elevated lung injury scores compared to recipients from RAGE −/− TBI donors

Acute lung injury scores (Fig. 4) were significantly lower in transplanted lungs from wildtype control donors (Fig. 4A) at 0.12 ± 0.02 when compared to TBI donors with a mean score of 0.44 ± 0.08 ($p < 0.01$, Fig. 4B). The means scores in transplanted lungs from TBI RAGE −/− donors was 0.17 ± 0.03 (minimal injury) and these lungs were otherwise histologically normal (Fig. 4C, D). This score was significantly lower than that for the wildtype C57BL/6 donor group ($p < 0.01$). Such results demonstrate that eliminating RAGE appears to preserve pulmonary injury post-transplantation.

Elevated IL-10 in TBI RAGE−/− Mice and Recipients of Lungs from TBI RAGE−/− Mice

IL-4, IL-6, IL-17a, TNF-α, and IFNγ BAL levels did not differ among donor sham-injured controls, TBI wildtype, and TBI RAGE −/− donor mice (Fig 5A–E). However, RAGE −/− donor mice had significantly higher levels of the anti-inflammatory molecule, IL-10, in BAL fluid (MFI 530.0 ± 23) when compared with sham controls (MFI 331.5 ±16) or TBI wildtype mice (MFI 408.5 ±13) ($p<0.01$) (Fig. 5F). Cytokine profiling was also determined in BAL fluid of transplanted lungs of mice whose donors were either TBI wildtype or RAGE

−/− mice. These transplants were performed 24 hours after sham or TBI. Cytokine profiling in the BAL fluid of recipients 8 hours post-transplant revealed no differences in IL-4, IL-6, IFNγ, TNF-α, and between wildtype and RAGE−/− donor lungs (Fig. 5A,B,D,E). IL-17a was significantly lower in the BAL fluid of recipients when the left lung was derivedfrom a RAGE −/− TBI mice: 245 ± 63.4 versus 602 ± 33.2 for TBI wildtype C57BL/6 control mice ($p<0.01$, Fig. 5C). Similar to observations in mice subjected to TBI alone, IL-10 was significantly elevated in BAL from transplanted lungs from RAGE −/− TBI donors compared to transplanted lungs from wildtype C57BL/6 TBI donors (1846 ± 19.6 versus 1241 ± 21.3, $p<0.01$, Fig. 5F).

HMGB1 Stimulates NF-κB Activation in Airway Epithelial Cells

In an effort to determine the downstream signaling pathways activated by HMGB1 binding to RAGE in the lungs, we stimulated rat alveolar type 2 epithelial cells with increasing concentrations of the non-oxidized (all-thiol) form of HMGB1 that binds only to RAGE. Translocation of NF-κB p65 and p50 from the cytoplasm to the nucleus, an indication of NF-κB activation, was enhanced 24 hours after stimulating AT2 cells with at least 10μg/mL of HMGB1 (Fig. 6).

Elevated donor HMGB1 correlates with poor blood oxygenation before and after human lung transplant

Blood was collected from human brain dead donors prior to procuring lungs to be utilized for bilateral lung transplants. Donor, recipient, and surgery specific characteristics are presented in Table 1. All blood samples were obtained from brain dead organ donors: 11 of the 18 died from TBI, the rest died of other causes including 4 from anoxia and 3 from stroke. The correlation between donor serum HMGB1 concentrations and the highest PaO2/FiO2ratio prior to procurement was determined. HMGB1 concentrations correlated inversely with donor PaO2/FiO2 ratios, where high HMGB1 levels were associated with lower PAO2/FIO2 ratios ($p<0.01$, Fig. 7A). This correlation was maintained when the data included only the subset of 11 donors that died from TBI ($p=0.05$, Fig. 7B). To examine the association between donor HMGB1 and recipient lung function, donor HMGB1 serum concentrations were correlated with recipient PaO2/FiO2ratios 48 hours after lung transplant. Linear regression revealed that donor HMGB1 concentrations also correlated inversely with recipient PaO2/FiO2ratios 48 hours after transplant, both in the 18 brain dead donors ($p<0.01$) as well as in the 11 TBI donors ($p<0.01$, Fig. 7C, D).

Discussion

Our results demonstrate that the HMGB1-RAGE ligand-receptor pathway serves as a central signal transduction mechanism for pulmonary dysfunction after TBI. TBI induced alterations in physiology and histology included reduced systemic arterial oxygen, decreased lung compliance, and pathology consistent with acute lung injury. These findings were RAGE-dependent as systemic oxygenation, lung compliance, and histology were restored almost completely to baseline in RAGE−/− mice subjected to TBI. Considering that a majority of lungs utilized for transplant are obtained from patients who have suffered a TBI, factors such as donor HMGB1 serum concentration may be predictive of lung function

before and after transplantation. Our current clinical data suggest that brain injury-induced HMGB1 release may have a role in donor and short-term recipient pulmonary function as well.

It is well established that pro-inflammatory molecules including HMGB1 are ligands for RAGE (25). Though initial reports suggested that extracellular HMGB1 released by necrotic and inflammatory cells functions as a late-acting cytokine mediating endotoxin-related lethality in mice (26) and cytokine synthesis in monocytes (27), there has been greater recognition that the effect of HMGB1 activation of RAGE has acute effects on leukocyte chemotaxis and vascular barrier disruption (28–30). Moreover, these effects may be important for sustaining inflammatory disease conditions alone (22) or in combination with toll-like receptors (31–34). Furthermore, our results with HMGB1 cortical staining demonstrating HMGB1 translocation from the nucleus after TBI agrees with reports demonstrating HMGB1 translocation and release after brain insult (35).

A recent report demonstrated that neutralization of HMGB1 may be a new treatment for brain injured animals due to reductions in brain edema and inflammation (36). Given our results, these beneficial effects can now be extended to the lungs. Given the ability of HMGB1 to bind to both RAGE and TLR4, our experimental outcomes implicate a pronounced role for RAGE as the lung dysfunction was more pronounced in the setting of TLR4 deficiency as compared to RAGE deficiency. One interpretation suggests that HMGB1-RAGE is instrumental for leukocyte infiltration while HMGB1-TLR4 may be responsible for cytokine production (37–40). Alternatively, it is known that HMGB1 can exist in either of two isoforms, all-thiol and disulfide, which have varying specificity for RAGE and TLR4. The all-thiol state of the isoform is first released into the extracellular space where it binds to RAGE and initiates chemoattraction of leukocytes (41). In contrast, the disulfide isoform exhibits a high affinity for TLR4 and induces the release of proinflammatory cytokines and mediators (42). Compared to the half-life of all-thiol (~17 minutes), the disulfide isoform's half life is significantly longer (up to 10 hours) (43). Considering the kinetic differences between the isoforms and the rapid induction of lung injury post TBI, it is apparent that the all-thiol form of HMGB1 binding to RAGE may be the primary pathway of lung injury in the current study. This finding is also supported by our data showing that the all-thiol form of HMGB1 induced NF-κB activation in airway epithelial cells. However, the exact contribution of both HMGB1 isoforms in TBI-induced lung injury is yet to be established.

The effects of the TAT-4BB decoy peptide and its ability to modulate TBI-induced inflammation is likely dependent on the adapter proteins common to both TLR4 and RAGE (22), though there is a suggestion that the HMGB1-TLR4-RAGE interaction is central to the downstream signaling (44). However, given the apparent commonality of downstream signaling for both TLR4 and RAGE, we hypothesize that decoy peptides would inhibit TBI-associated changes in pulmonary tissue and physiology regardless of the signaling receptor.

Ligand-dependent activation of RAGE may modulate chemotactic actions of leukocytes. Our results reinforce prior reports that HMGB1 may stimulate RAGE activation of NF-κB (45), so it is conceivable that pulmonary dysfunction following TBI include the production of pro-

inflammatory cytokines such as IL-6, TGF-β and IL-17a (45–48). However, the only cytokine that appeared to be altered in the BAL following injury was the anti-inflammatory cytokine, IL-10. Together with previous observations in a model of hemorrhagic shock (49) and a recent report suggesting that signaling via RAGE is linked to downregulation of IL-10, it appears that modulation of this important anti-inflammatory cytokine is regulated by RAGE activation. More importantly, it is possible that increased IL-10 concentrations could dampen the inflammatory process and mitigate injury to the pulmonary system. An example of such an effect may be evidenced by the beneficial effects of soluble RAGE administration in IL-10 null mice subjected to chronic colonic inflammation (50). In addition, IL-10 gene therapy has been utilized to repair donor human lungs prior to transplantation (51).

Other work using an ischemia reperfusion injury model demonstrated that the HMGB1-RAGE pathway contributes to IL-17a production from invariant natural killer cells, which are crucial for the initiation of ischemia reperfusion injury (17). Our results corroborated this concept of HMGB1-RAGE mediated effects on cytokine production in ischemia reperfusion injury We observed decreased IL-17a protein expression in the BAL of recipients of RAGE −/− TBI donor lungs as compared to recipients of wildtype TBI donor lungs. Additionally, the connection between RAGE and lung dysfunction has been studied outside of the setting of TBI. Circulating soluble RAGE was reported to be a marker of primary graft dysfunction, which is a form of ischemia reperfusion injury that occurs after lung transplantation (52).

Non-cytokine pathways have also been linked to TBI-induced lung injury. A recent report implicated high levels of glutamate after brain injury triggering acute lung injury mediated through interaction of the adenosine A2A receptor and the metabotropic glutamate receptor 5 (mGluR5) on bone marrow-derived cells (53). This pathway may run in parallel to the HMGB1-RAGE axis with overlap of downstream signaling.

In summary, the current study demonstrates a mechanism of TBI-induced acute lung injury that includes a key role for the HMGB1-RAGE pathway. These data may be important for preventing pulmonary complications in patients after TBI. These findings could also have implications in the field of lung transplantation. Most lungs for transplantation are procured from patients after TBI. Remarkably, only 15–20% of such lungs are suitable for transplant due to abnormal physiology that includes impaired oxygenation, a critical parameter of lung function. Given that TBI has profound detrimental effects on pulmonary physiology, the current study suggests that targeting the RAGE-HMGB1 axis could serve as a new therapeutic approach to increase the quality of lungs suitable for transplantation.

Materials and Methods

Study Design

This study was designed to identify the role of the HMGB1-RAGE inflammatory pathway in TBI-induced pulmonary dysfunction. To do this, we utilized murine models of traumatic brain injury and lung transplantation in wildtype and transgenic mice as further described below to better understand the pathways at work. We also administered an HMGB1 neutralizing antibody as well as a downstream signaling decoy peptide to further delineate the downstream signaling. Additionally, we utilized our institution’s prospectively collected

lung transplant biobank to correlate donor levels of HMGB1 with donor and recipient lung function.

Human Studies

All human studies were approved by the Indiana University Institutional Review Board. Additionally, all lung transplant recipients consented and all donor families consented for organ donation and research. Using a prospectively collected samples from lung transplant recipients and donors, we identified donor cause of death and donor serum levels of HMGB1 using an ELISA kit (IBL International, Hamburg, Germany) and correlated with donor pulmonary function values and short-term recipient pulmonary values and outcomes.

Animals

All mice were housed in the Laboratory Animal Resource Center at Indiana University School of Medicine in accordance with institutional guidelines. All mice were 8–12 weeks of age and 24–32g and used as both donors and recipients. Mice were randomly assigned to groups. All studies were approved by the Laboratory Animal Resource Center at the Indiana University School of Medicine. Specific pathogen-free male inbred mice C57BL/6 were purchased from Harlan Sprague-Dawley (Indianapolis, IN). TLR4 −/− mice were purchased from Jackson Laboratory (Bar Harbor, ME) and RAGE −/− mice were obtained from onsite colonies (54).

Traumatic Brain Injury (TBI)

Mice were subjected either to a TBI using a controlled cortical impact model using an electromagnetic impactor (Impactor One™, MyNeuroLab) or sham-injury (55). The mice were anesthetized with isoflurane and ketamine and placed in a stereotaxic frame (Kopf Instruments, Tujunga, CA). The skull was exposed in the left fronto-pareital cortex using an electric drill. Prior to the injury, the impacting piston was angled so that the impacting tip (3 mm in diameter) was perpendicular to the exposed cortical surface. This was accomplished by rotating the entire stereotaxic frame on the transverse plane. Sham control animals were exposed to anesthesia, skull exposure, and suturing without the cortical impact. The amount of deformation was set at either 0.5 mm (moderate injury) or 1.0 mm (severe injury). After injury, animals were allowed to recover and were able to eat and drink for 4–24 hours prior to harvest.

Serum and BAL

After euthanization, blood was obtained from the right ventricle and centrifuged (15 min; 1500g; 4°C) and serum was isolated. For bronchoalveolar lavage (BAL), lungs were lavaged with aliquots totaling 3 ml of Ca2+- and Mg2+-free PBS supplemented with 0.1 mM EDTA. Samples were centrifuged (10 min; 1500g; 4°C).

Pulmonary Function Tests and Arterial Blood Gases

After inducing anesthesia with 1–2% Isoflurane, all mice were mechanically ventilated with a rodent ventilator using room air, at a rate of 140 breaths per minute, a tidal volume of 0.3 ml, and 2 cmH2O of positive end-expiratory pressure. The animals were placed on a heated

(37C°) pad and pulmonary function tests were then performed with the Flexi Vent system (Scireq, Montreal, PQ, Canada). At the competition of pulmonary function testing, a 25 gauge angiocatheter was placed at the junction of the left ventricle and ascending aorta and 2–3 mL of arterial blood was obtained. This was run on an iSTAT point-of-care analyzer (Abbott Laboratories, Princeton, NJ). Subsequently, mice were euthanized and lungs harvested in 10% neutral buffered formalin.

Histology and Lung Injury Scoring

After mice were euthanized, native and donor lungs were harvested, glutaraldehyde-fixed, and paraffin embedded. A portion of the each lobe of each lung was sectioned and stained with hematoxylin and eosin. Lungs were stained with hematoxylin and eosin and scored by a blinded pathologist using the Lung Injury Scoring System from the American Thoracic Society Workshop Report (19). This criteria gives a continuous score between 0 (no injury) and 1 (severe injury). Additionally, immunohistochemistry was performed on lung sections for Caspase-3, a marker of apoptosis.

Myeloperoxidase Levels in BAL

BAL fluid from animals was collected and myeloperoxidase (MPO) levels were measured using an ELISA kit (Cell Sciences, Canton, MA) according to manufacturer's instructions.

PET/CT Cardiac Output and Image Analysis

Cardiac output was calculated using Dynamic high resolution 18F-NaF Positron Emission Tomography (PET) Computed Topography (CT). Subsequently, CT and PET images were co-registered for image analysis and the Stewart-Hamitlon indicator dilution method was used to calculate cardiac output using a left ventricular time activity curve. The full details are available in the supplemental material.

TAT-4BB Decoy Peptide

TAT-4BB was obtained from GenScript (Piscataway, NJ) containing the essential amino acid sequence of the TAT domain with 4BB (YGRKKRRQRRR-LHYRDRIPGVAIAA). This was administered via a subcutaneous 24 hour micro-osmotic pump from Alzert (Cupertino, CA). Vehicle was used as a negative control.

Serum HMGB1 Measurement

HMGB1 serum levels were determined by using an ELISA kit (IBL International, Hamburg, Germany) according to manufacturer's instructions.

HMGB1 Neutralizing Antibody

Neutralization of HMGB1 was accomplished by administering anti-HMGB1 chicken IgY neutralizing polyclonal antibody (IBL International, Toronto, ON) dosed at 2mg/kg both 30 minutes prior to TBI. Isotype matched control antibodies were administered to control animals with the same dosing regimen. Additionally, immunohistochemistry was performed on paraffin-embedded mouse lungs against HMGB1 (ab18256**,** Abcam, Cambridge, MA) as previously described (56). Brain tissue was also stained was also performed using

immunocytochemical and immunohistochemical methodologies previously described (57). Cortical tissue was serially sectioned at 14 μm and was used in immunohistochemical experiments. The primary antisera used was the rabbit anti-HMGB1 antibody (1:1,000; Sigma Aldrich). Sections were incubated in secondary donkey ant-Rabbit conjugated to CY3 (Jackson ImmunoResearch Laboratories, Inc., West Grove, PA, USA). Nuclear co-localization with DAPI was also performed and images were imported into Image-Pro Plus (Media Cybernetics, Silver Spring, MD, USA) for quantification.

HMGB1 Stimulated NF-κB Activation in Airway Epithelial Cells

A cell culture of rat alveolar type 2 (AT2) cells were stimulated with increasing concentrations of non-oxidizable LPS-free HMGB1 (HMGBiotech, Milan, Italy) at 0, 5, 10, and 15ug/mL for 24 hours. Nuclear and cytosolic protein lysates were then collected and analyzed for p50 and p65 NF-κB by Western blot analysis. Further details are supplied in the supplemental materials.

Cytokine profiling by cytometric bead array (CBA)

BAL fluid from animals was collected and cytokine protein levels of IL-17A, IL-10, TNF-α, IFN-γ, IL-6, IL-4, and IL-2 were measured using the Mouse Th1/Th2/Th17 Cytokine Kit (BD Biosciences, San Jose, CA) according to manufacturer's instructions.

Murine Orthotopic Left Lung Transplantation

All surgical procedures were performed utilizing sterile techniques in a previously described method (58) which is detailed in the supplemental materials.

Statistical Analysis

Data were normally distributed and analyzed statistically with GraphPad Prism (GraphPad Software Inc., San Diego, CA). Results are expressed as means ± SEM. Differences between groups were analyzed by unpaired t-tests and analysis of variance and Tukey post hoc test. Correlation coefficient between two variables was calculated with the Pearson correlation test. *P* values not exceeding 0.05 were considered significant.

Supplementary Material

Refer to Web version on PubMed Central for supplementary material.

Acknowledgments

We would like to acknowledge the work and assistance of the Indiana Organ Procurement Organization in assisting with our clinical donor information.

Funding: This work was supported by National Institute of Health grants R01 HL096845, and NIAID P01AI084853 to DSW; R01 DK100905 and Indiana Spinal Cord and Brain Injury Research Fund to FAW

References

1. Bittle GJ, Sanchez PG, Kon ZN, Claire Watkins A, Rajagopal K, Pierson RN 3rd, Gammie JS, Griffith BP. The use of lung donors older than 55 years: a review of the United Network of Organ

Sharing database. The Journal of heart and lung transplantation : the official publication of the International Society for Heart Transplantation. 2013; 32:760–768.

2. Cypel M, Keshavjee S. Strategies for safe donor expansion: donor management, donations after cardiac death, ex-vivo lung perfusion. Current opinion in organ transplantation. 2013
3. Davison DL, Terek M, Chawla LS. Neurogenic pulmonary edema. Crit Care. 2012; 16:212. [PubMed: 22429697]
4. Rincon F, Ghosh S, Dey S, Maltenfort M, Vibbert M, Urtecho J, McBride W, Moussouttas M, Bell R, Ratliff JK, Jallo J. Impact of acute lung injury and acute respiratory distress syndrome after traumatic brain injury in the United States. Neurosurgery. 2012; 71:795–803. [PubMed: 22855028]
5. Yang H, Antoine DJ, Andersson U, Tracey KJ. The many faces of HMGB1: molecular structure-functional activity in inflammation, apoptosis, and chemotaxis. J Leukoc Biol. 2013; 93:865–873. [PubMed: 23446148]
6. Maroso M, Balosso S, Ravizza T, Liu J, Aronica E, Iyer AM, Rossetti C, Molteni M, Casalgrandi M, Manfredi AA, Bianchi ME, Vezzani A. Toll-like receptor 4 and high-mobility group box-1 are involved in ictogenesis and can be targeted to reduce seizures. Nat Med. 2010; 16:413–419. [PubMed: 20348922]
7. Feldman P, Due MR, Ripsch MS, Khanna R, White FA. The persistent release of HMGB1 contributes to tactile hyperalgesia in a rodent model of neuropathic pain. J Neuroinflammation. 2012; 9:180. [PubMed: 22824385]
8. Andersson U, Tracey KJ. HMGB1 is a therapeutic target for sterile inflammation and infection. Annu Rev Immunol. 2011; 29:139–162. [PubMed: 21219181]
9. Sims GP, Rowe DC, Rietdijk ST, Herbst R, Coyle AJ. HMGB1 and RAGE in inflammation and cancer. Annu Rev Immunol. 2010; 28:367–388. [PubMed: 20192808]
10. Rouhiainen A, Kuja-Panula J, Tumova S, Rauvala H. RAGE-mediated cell signaling. Methods Mol Biol. 2013; 963:239–263. [PubMed: 23296615]
11. Iori V, Maroso M, Rizzi M, Iyer AM, Vertemara R, Carli M, Agresti A, Antonelli A, Bianchi ME, Aronica E, Ravizza T, Vezzani A. Receptor for Advanced Glycation Endproducts is upregulated in temporal lobe epilepsy and contributes to experimental seizures. Neurobiol Dis. 2013; 58:102–114. [PubMed: 23523633]
12. Buckley ST, Ehrhardt C. The receptor for advanced glycation end products (RAGE) and the lung. Journal of biomedicine & biotechnology. 2010; 2010:917108. [PubMed: 20145712]
13. Bopp C, Bierhaus A, Hofer S, Bouchon A, Nawroth PP, Martin E, Weigand MA. Bench-to-bedside review: The inflammation-perpetuating pattern-recognition receptor RAGE as a therapeutic target in sepsis. Crit Care. 2008; 12:201. [PubMed: 18226173]
14. Bierhaus A, Humpert PM, Morcos M, Wendt T, Chavakis T, Arnold B, Stern DM, Nawroth PP. Understanding RAGE, the receptor for advanced glycation end products. J Mol Med (Berl). 2005; 83:876–886. [PubMed: 16133426]
15. Fiuza C, Bustin M, Talwar S, Tropea M, Gerstenberger E, Shelhamer JH, Suffredini AF. Inflammation-promoting activity of HMGB1 on human microvascular endothelial cells. Blood. 2003; 101:2652–2660. [PubMed: 12456506]
16. Treutiger CJ, Mullins GE, Johansson AS, Rouhiainen A, Rauvala HM, Erlandsson-Harris H, Andersson U, Yang H, Tracey KJ, Andersson J, Palmblad JE. High mobility group 1 B-box mediates activation of human endothelium. J Intern Med. 2003; 254:375–385. [PubMed: 12974876]
17. Sharma AK, Lapar DJ, Stone ML, Zhao Y, Kron IL, Laubach VE. Receptor for Advanced Glycation End Products (RAGE) on iNKT Cells Mediates Lung Ischemia-Reperfusion Injury. Am J Transplant. 2013; 13:2255–2267. [PubMed: 23865790]
18. Qin S, Wang H, Yuan R, Li H, Ochani M, Ochani K, Rosas-Ballina M, Czura CJ, Huston JM, Miller E, Lin X, Sherry B, Kumar A, Larosa G, Newman W, Tracey KJ, Yang H. Role of HMGB1 in apoptosis-mediated sepsis lethality. J Exp Med. 2006; 203:1637–1642. [PubMed: 16818669]
19. Matute-Bello G, Downey G, Moore BB, Groshong SD, Matthay MA, Slutsky AS, Kuebler WM. G Acute Lung Injury in Animals Study. An official American Thoracic Society workshop report: features and measurements of experimental acute lung injury in animals. Am J Respir Cell Mol Biol. 2011; 44:725–738. [PubMed: 21531958]

20. Kawai T, Akira S. The role of pattern-recognition receptors in innate immunity: update on Toll-like receptors. Nature immunology. 2010; 11:373–384. [PubMed: 20404851]
21. Toshchakov VY, Szmacinski H, Couture LA, Lakowicz JR, Vogel SN. Targeting TLR4 Signaling by TLR4 Toll/IL-1 Receptor Domain-Derived Decoy Peptides: Identification of the TLR4 Toll/IL-1 Receptor Domain Dimerization Interface. Journal of immunology. 2011; 186:4819–4827.
22. Sakaguchi M, Murata H, Yamamoto K, Ono T, Sakaguchi Y, Motoyama A, Hibino T, Kataoka K, Huh NH. TIRAP, an adaptor protein for TLR2/4, transduces a signal from RAGE phosphorylated upon ligand binding. PLoS One. 2011; 6:e23132. [PubMed: 21829704]
23. Putranto EW, Murata H, Yamamoto K, Kataoka K, Yamada H, Futami J, Sakaguchi M, Huh NH. Inhibition of RAGE signaling through the intracellular delivery of inhibitor peptides by PEI cationization. International journal of molecular medicine. 2013; 32:938–944. [PubMed: 23934084]
24. Toshchakov VU, Basu S, Fenton MJ, Vogel SN. Differential involvement of BB loops of toll-IL-1 resistance (TIR) domain-containing adapter proteins in TLR4-versus TLR2-mediated signal transduction. Journal of immunology. 2005; 175:494–500.
25. Bierhaus A, Haslbeck KM, Humpert PM, Liliensiek B, Dehmer T, Morcos M, Sayed AA, Andrassy M, Schiekofer S, Schneider JG, Schulz JB, Heuss D, Neundorfer B, Dierl S, Huber J, Tritschler H, Schmidt AM, Schwaninger M, Haering HU, Schleicher E, Kasper M, Stern DM, Arnold B, Nawroth PP. Loss of pain perception in diabetes is dependent on a receptor of the immunoglobulin superfamily. The Journal of clinical investigation. 2004; 114:1741–1751. [PubMed: 15599399]
26. Wang HC, Bloom O, Zhang MH, Vishnubhakat JM, Ombrellino M, Che JT, Frazier A, Yang H, Ivanova S, Borovikova L, Manogue KR, Faist E, Abraham E, Andersson J, Andersson U, Molina PE, Abumrad NN, Sama A, Tracey KJ. HMG-1 as a late mediator of endotoxin lethality in mice. Science. 1999; 285:248–251. [PubMed: 10398600]
27. Andersson U, Wang H, Palmblad K, Aveberger AC, Bloom O, Erlandsson-Harris H, Janson A, Kokkola R, Zhang M, Yang H, Tracey KJ. High mobility group 1 protein (HMG-1) stimulates proinflammatory cytokine synthesis in human monocytes. J Exp Med. 2000; 192:565–570. [PubMed: 10952726]
28. Rouhiainen A, Kuja-Panula J, Wilkman E, Pakkanen J, Stenfors J, Tuominen RK, Lepantalo M, Carpen O, Parkkinen J, Rauvala H. Regulation of monocyte migration by amphoterin (HMGB1). Blood. 2004; 104:1174–1182. [PubMed: 15130941]
29. Yang D, Chen Q, Yang H, Tracey KJ, Bustin M, Oppenheim JJ. High mobility group box-1 protein induces the migration and activation of human dendritic cells and acts as an alarmin. J Leukoc Biol. 2007; 81:59–66. [PubMed: 16966386]
30. Wolfson RK, Chiang ET, Garcia JGN. HMGB1 induces human lung endothelial cell cytoskeletal rearrangement and barrier disruption. Microvascular Research. 2011; 81:189–197. [PubMed: 21146549]
31. van Zoelen MA, Yang H, Florquin S, Meijers JC, Akira S, Arnold B, Nawroth PP, Bierhaus A, Tracey KJ, van der Poll T. Role of toll-like receptors 2 and 4, and the receptor for advanced glycation end products in high-mobility group box 1-induced inflammation in vivo. Shock. 2009; 31:280–284. [PubMed: 19218854]
32. Hreggvidsdottir HS, Ostberg T, Wahamaa H, Schierbeck H, Aveberger AC, Klevenvall L, Palmblad K, Ottosson L, Andersson U, Harris HE. The alarmin HMGB1 acts in synergy with endogenous and exogenous danger signals to promote inflammation. J Leukoc Biol. 2009; 86:655–662. [PubMed: 19564572]
33. Hreggvidsdottir HS, Lundberg AM, Aveberger AC, Klevenvall L, Andersson U, Harris HE. High mobility group box protein 1 (HMGB1)-partner molecule complexes enhance cytokine production by signaling through the partner molecule receptor. Mol Med. 2012; 18:224–230. [PubMed: 22076468]
34. Sirois CM, Jin T, Miller AL, Bertheloot D, Nakamura H, Horvath GL, Mian A, Jiang J, Schrum J, Bossaller L, Pelka K, Garbi N, Brewah Y, Tian J, Chang C, Chowdhury PS, Sims GP, Kolbeck R, Coyle AJ, Humbles AA, Xiao TS, Latz E. RAGE is a nucleic acid receptor that promotes inflammatory responses to DNA. J Exp Med. 2013

35. Qiu J, Nishimura M, Wang Y, Sims JR, Qiu S, Savitz SI, Salomone S, Moskowitz MA. Early release of HMGB-1 from neurons after the onset of brain ischemia. Journal of cerebral blood flow and metabolism : official journal of the International Society of Cerebral Blood Flow and Metabolism. 2008; 28:927–938.

36. Okuma Y, Liu K, Wake H, Zhang J, Maruo T, Date I, Yoshino T, Ohtsuka A, Otani N, Tomura S, Shima K, Yamamoto Y, Yamamoto H, Takahashi HK, Mori S, Nishibori M. Anti-high mobility group box-1 antibody therapy for traumatic brain injury. Annals of neurology. 2012; 72:373–384. [PubMed: 22915134]

37. O'Neill LAJ. The interleukin-1 receptor/Toll-like receptor superfamily: 10 years of progress. Immunological Reviews. 2008; 226:10–18. [PubMed: 19161412]

38. Fitzgerald KA, Chen ZJ. Sorting out Toll signals. Cell. 2006; 125:834–836. [PubMed: 16751092]

39. Dinarello CA. Proinflammatory cytokines. Chest. 2000; 118:503–508. [PubMed: 10936147]

40. O'Neill L. The Toll/interleukin-1 receptor domain: a molecular switch for inflammation and host defence. Biochem Soc Trans. 2000; 28:557–563. [PubMed: 11044374]

41. Venereau E, Schiraldi M, Uguccioni M, Bianchi ME. HMGB1 and leukocyte migration during trauma and sterile inflammation. Mol Immunol. 2013; 55:76–82. [PubMed: 23207101]

42. Yang H, Lundback P, Ottosson L, Erlandsson-Harris H, Venereau E, Bianchi ME, Al-Abed Y, Andersson U, Tracey KJ, Antoine DJ. Redox modification of cysteine residues regulates the cytokine activity of high mobility group box-1 (HMGB1). Mol Med. 2012; 18:250–259. [PubMed: 22105604]

43. Zandarashvili L, Sahu D, Lee K, Lee YS, Singh P, Rajarathnam K, Iwahara J. Real-time kinetics of high-mobility group box 1 (HMGB1) oxidation in extracellular fluids studied by in situ protein NMR spectroscopy. J Biol Chem. 2013; 288:11621–11627. [PubMed: 23447529]

44. van Beijnum JR, Buurman WA, Griffioen AW. Convergence and amplification of toll-like receptor (TLR) and receptor for advanced glycation end products (RAGE) signaling pathways via high mobility group B1 (HMGB1). Angiogenesis. 2008; 11:91–99. [PubMed: 18264787]

45. Wu X, Mi Y, Yang H, Hu A, Zhang Q, Shang C. The activation of HMGB1 as a progression factor on inflammation response in normal human bronchial epithelial cells through RAGE/JNK/NF-kappaB pathway. Molecular and cellular biochemistry. 2013; 380:249–257. [PubMed: 23712703]

46. Luan ZG, Zhang H, Yang PT, Ma XC, Zhang C, Guo RX. HMGB1 activates nuclear factor-kappaB signaling by RAGE and increases the production of TNF-alpha in human umbilical vein endothelial cells. Immunobiology. 2010; 215:956–962. [PubMed: 20163887]

47. Qin YH, Dai SM, Tang GS, Zhang J, Ren D, Wang ZW, Shen Q. HMGB1 enhances the proinflammatory activity of lipopolysaccharide by promoting the phosphorylation of MAPK p38 through receptor for advanced glycation end products. Journal of immunology. 2009; 183:6244–6250.

48. Huttunen HJ, Fages C, Rauvala H. Receptor for advanced glycation end products (RAGE)-mediated neurite outgrowth and activation of NF-kappaB require the cytoplasmic domain of the receptor but different downstream signaling pathways. The Journal of biological chemistry. 1999; 274:19919–19924. [PubMed: 10391939]

49. Raman KG, Sappington PL, Yang R, Levy RM, Prince JM, Liu S, Watkins SK, Schmidt AM, Billiar TR, Fink MP. The role of RAGE in the pathogenesis of intestinal barrier dysfunction after hemorrhagic shock. Am J Physiol Gastrointest Liver Physiol. 2006; 291:G556–565. [PubMed: 16751175]

50. Hofmann MA, Drury S, Fu C, Qu W, Taguchi A, Lu Y, Avila C, Kambham N, Bierhaus A, Nawroth P, Neurath MF, Slattery T, Beach D, McClary J, Nagashima M, Morser J, Stern D, Schmidt AM. RAGE mediates a novel proinflammatory axis: a central cell surface receptor for S100/calgranulin polypeptides. Cell. 1999; 97:889–901. [PubMed: 10399917]

51. Cypel M, Liu M, Rubacha M, Yeung JC, Hirayama S, Anraku M, Sato M, Medin J, Davidson BL, de Perrot M, Waddell TK, Slutsky AS, Keshavjee S. Functional repair of human donor lungs by IL-10 gene therapy. Sci Transl Med. 2009; 1:4ra9.

52. Christie JD, Shah CV, Kawut SM, Mangalmurti N, Lederer DJ, Sonett JR, Ahya VN, Palmer SM, Wille K, Lama V, Shah PD, Shah A, Weinacker A, Deutschman CS, Kohl BA, Demissie E, Bellamy S, Ware LB, Lung G. Transplant Outcomes, Plasma levels of receptor for advanced

glycation end products, blood transfusion, and risk of primary graft dysfunction. American journal of respiratory and critical care medicine. 2009; 180:1010–1015. [PubMed: 19661249]

53. Dai SS, Wang H, Yang N, An JH, Li W, Ning YL, Zhu PF, Chen JF, Zhou YG. Plasma glutamate-modulated interaction of A2AR and mGluR5 on BMDCs aggravates traumatic brain injury-induced acute lung injury. J Exp Med. 2013; 210:839–851. [PubMed: 23478188]
54. Liliensiek B, Weigand MA, Bierhaus A, Nicklas W, Kasper M, Hofer S, Plachky J, Grone HJ, Kurschus FC, Schmidt AM, Yan SD, Martin E, Schleicher E, Stern DM, Hammerling GG, Nawroth PP, Arnold B. Receptor for advanced glycation end products (RAGE) regulates sepsis but not the adaptive immune response. J Clin Invest. 2004; 113:1641–1650. [PubMed: 15173891]
55. Brittain JM, Chen L, Wilson SM, Brustovetsky T, Gao X, Ashpole NM, Molosh AI, You H, Hudmon A, Shekhar A, White FA, Zamponi GW, Brustovetsky N, Chen J, Khanna R. Neuroprotection against traumatic brain injury by a peptide derived from the collapsin response mediator protein 2 (CRMP2). J Biol Chem. 2011; 286:37778–37792. [PubMed: 21832084]
56. Zampell JC, Yan A, Avraham T, Andrade V, Malliaris S, Aschen S, Rockson SG, Mehrara BJ. Temporal and spatial patterns of endogenous danger signal expression after wound healing and in response to lymphedema. American journal of physiology Cell physiology. 2011; 300:C1107–1121. [PubMed: 21248077]
57. Bhangoo S, Ren D, Miller RJ, Henry KJ, Lineswala J, Hamdouchi C, Li B, Monahan PE, Chan DM, Ripsch MS, White FA. Delayed functional expression of neuronal chemokine receptors following focal nerve demyelination in the rat: a mechanism for the development of chronic sensitization of peripheral nociceptors. Molecular pain. 2007; 3:38. [PubMed: 18076762]
58. Fan L, Benson HL, Vittal R, Mickler EA, Presson R, Fisher AJ, Cummings OW, Heidler KM, Keller MR, Burlingham WJ, Wilkes DS. Neutralizing IL-17 prevents obliterative bronchiolitis in murine orthotopic lung transplantation. Am J Transplant. 2011; 11:911–922. [PubMed: 21521466]
59. Rouze NC, Schmand M, Siegel S, Hutchins GD. Design of a Small Animal PET Imaging System With 1 Microliter Volume Resolution. IEEE TRANSACTIONS ON NUCLEAR SCIENCE. 2004; 51:757–763.
60. Soon VC, Miller MA, Hutchins GD. A non-iterative method for emission tomographic image reconstruction with resolution recovery. Nuclear Science Symposium Conference. 2007:3468–3473. Record.
61. Kreissl MC, Wu HM, Stout DB, Ladno W, Schindler TH, Zhang XL, Prior JO, Prins ML, Chatziioannou AF, Huang SC, Schelbert HR. Noninvasive measurement of cardiovascular function in mice with high-temporal-resolution small-animal PET. Journal of Nuclear Medicine. 2006; 47:974–980. [PubMed: 16741307]
62. Studholme C, Hawkes DJ, Hill DL. Normalized entropy measure for multimodality image alignment. Proc SPIE Medical Imaging. 1998; 3338:132–143.
63. Profant M, Vyska K, Eckhardt U. The Stewart-Hamilton Equations and the Indicator Dilution Method. SIAM Journal on Applied Mathematics. 1978; 34:666–675.

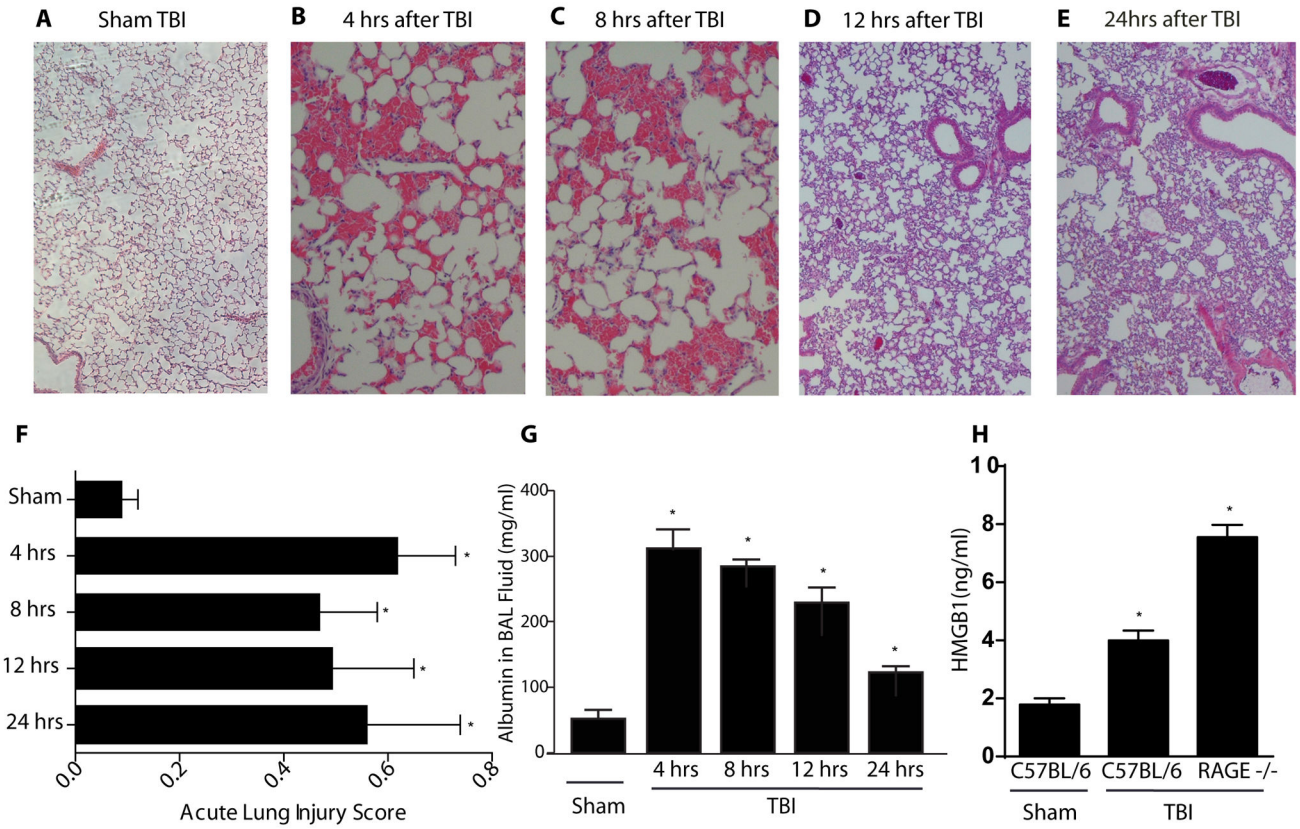

Figure 1.

Acute lung injury in C57BL/6 mice 4–24 hours after TBI. Representative H/E histology sections of C57BL/6 mouse lungs after traumatic brain injury at various time points. (**A**) Control animals with sham TBI. (**B**) 4 hours after TBI with alveolar hemorrhage. (**C**) 8 hours after TBI with alveolar hemorrhage. (**D**) 12 hours after TBI with interstitial neutrophils. (**E**) 24 hours after TBI with interstitial neutrophils. (**F**) Acute lung injury scores from a blinded pathologist based on a standardized scoring system from the American Thoracic Society (19). Scores are continuous between 0 and 1 with 0 representing no injury and 1 representing severe acute lung injury. (**G**) Albumin concentrations in BAL fluid after TBI. (**H**) Systemic concentrations of HMGB1 24 hours after severe TBI in the sham injured group as well as in C57BL/6 and RAGE −/− mice 24 hours after TBI. n=6–8 per condition, Student's t test comparison with the reference sham injured group, comparisons versus sham-injured group, *p<0.01.

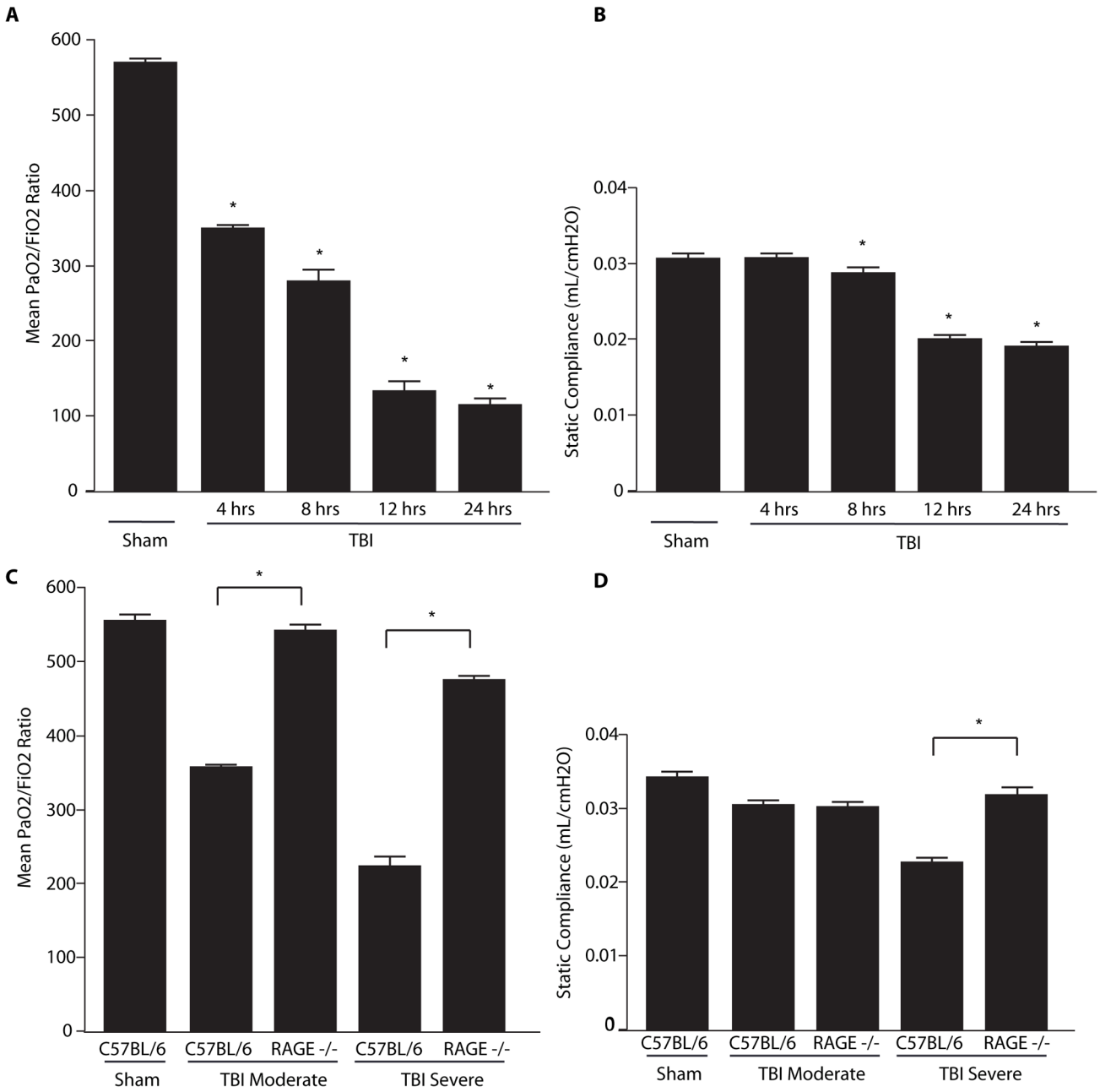

Figure 2.

PaO2/FiO2 ratios and compliance values derived from C57BL/6 and RAGE −/−mice 4–24 hours after TBI. (**A**) PaO2/FiO2 ratios from controls without TBI and wildtype mice 4–24 hours after TBI. (**B**) Static compliance values obtained via Pulmonary Function Testing from controls without TBI and wildtype mice 4–24 hours after TBI. (**C**) PaO2/FiO2 ratios from C57BL/6 and RAGE−/− 24 hours after TBI. Animals were administered either moderate or severe TBI. (**D**) Compliance values from controls and C57BL/6 and RAGE −/− mice 24 hours after TBI. n=4–7 mice per condition, comparisons versus sham-injured group unless

otherwise indicated, *p<0.01 Statistical testing included unpaired t-tests and analysis of variance.

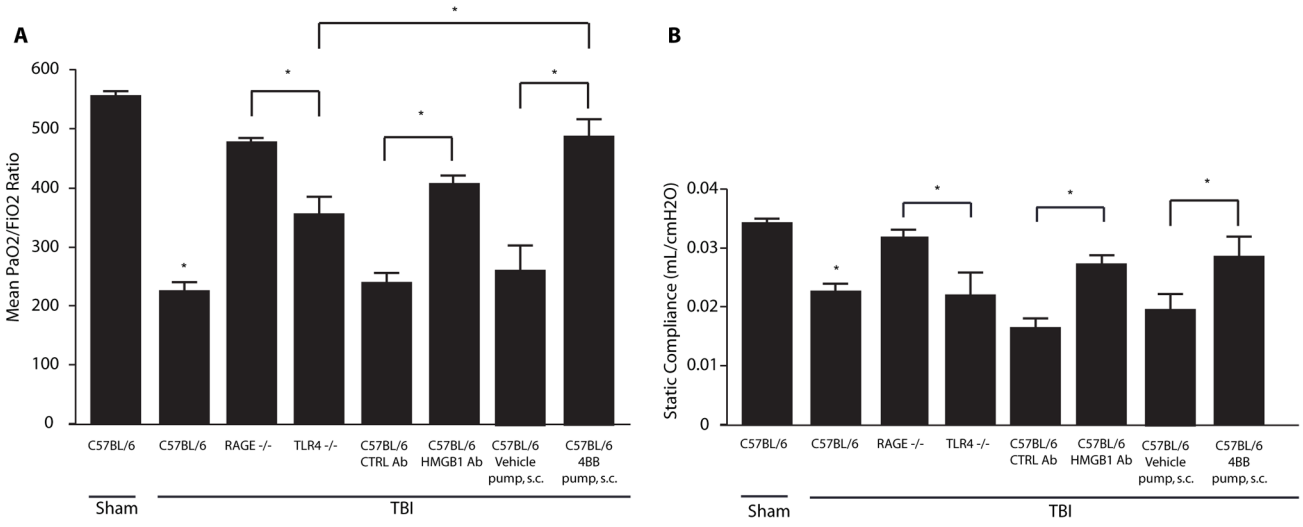

Figure 3.

PaO2/FiO2 ratios and compliance values 24 hours after TBI in RAGE −/−, TLR4 −/− mice treated with HMGB1 neutralizing antibody, and mice treated with TAT-4BB decoy peptide. (**A**) PaO2/FiO2 ratios in control mice and RAGE −/−, TLR4 −/− mice treated with HMGB1 antibody or control antibody, or treated with 4BB (Myd-88) decoy peptide 24 hours after TBI. (**B**) Compliance values in RAGE −/−, TLR4 −/− mice treated with HMGB1 antibody or control antibody, or with 4BB decoy peptide 24 hours after TBI. n=5–7 per condition, comparisons versus sham-injured group unless otherwise indicated, *p≤0.01. Statistical testing included unpaired t-tests and analysis of variance.

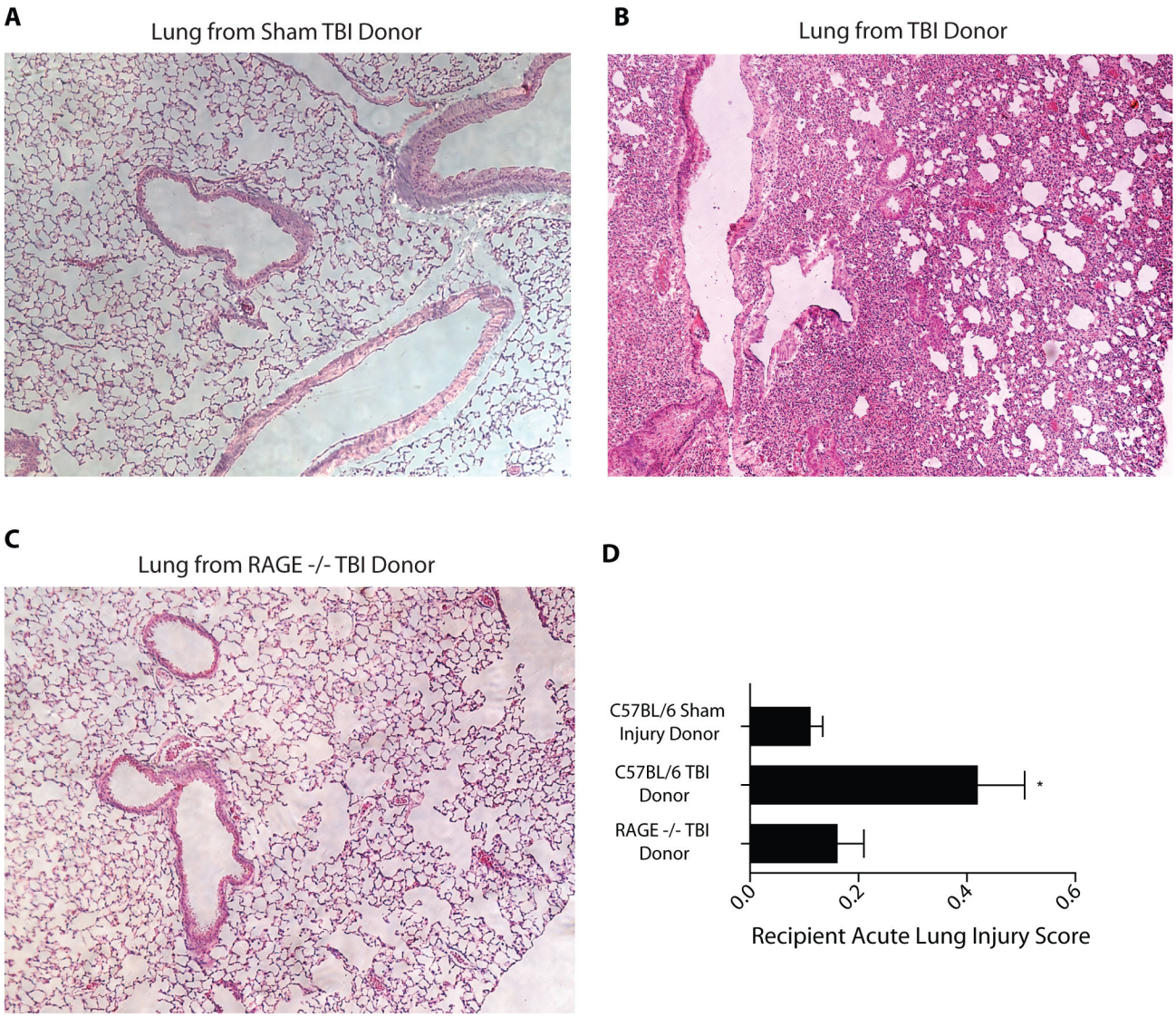

Figure 4.

Histology and acute lung injury scores for transplanted left lungs from control donor mice, wildtype TBI donor mice, or RAGE−/− TBI donor mice. Representative H/E histology sections from transplanted lungs 5 days after transplant. (**A**) Transplanted left lung from healthy donor with sham TBI. (**B**) Transplanted left lung from wildtype TBI donor. (**C**) Transplanted left lung from RAGE−/− TBI donor. (**D**) Acute lung injury scores from transplant recipients who received lungs from three different donors: wildtype animals with sham TBI, wildtype animals with TBI, and RAGE −/− donors with TBI. n=6–8 per condition, comparison versus sham-injured group, *p<0.01. Statistical testing included unpaired t-tests and analysis of variance

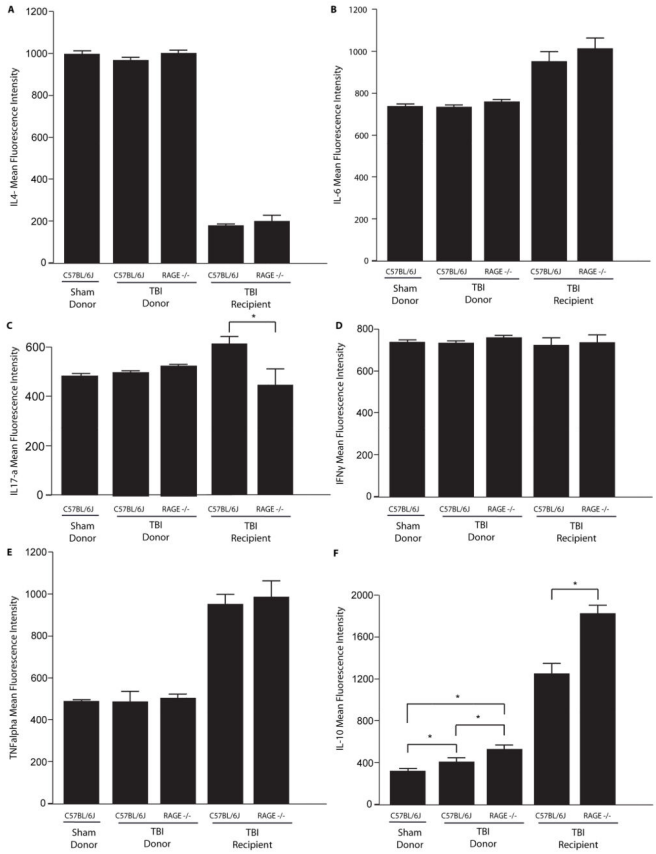

Figure 5.

BAL cytokine profiles in control and injured donor mice 24 hours after TBI. Cytokine profiling was also performed in left lung transplant recipients of TBI donor lungs 8 hours after transplant. (**A–F**) Mean Fluorescence Intensity of IL-4, IL-6, IL-17a, IFN-γ, TNF-α, IL-17A, and IL-10. n=5–7 per condition, *p<0.01. Statistical testing included unpaired t-tests and analysis of variance

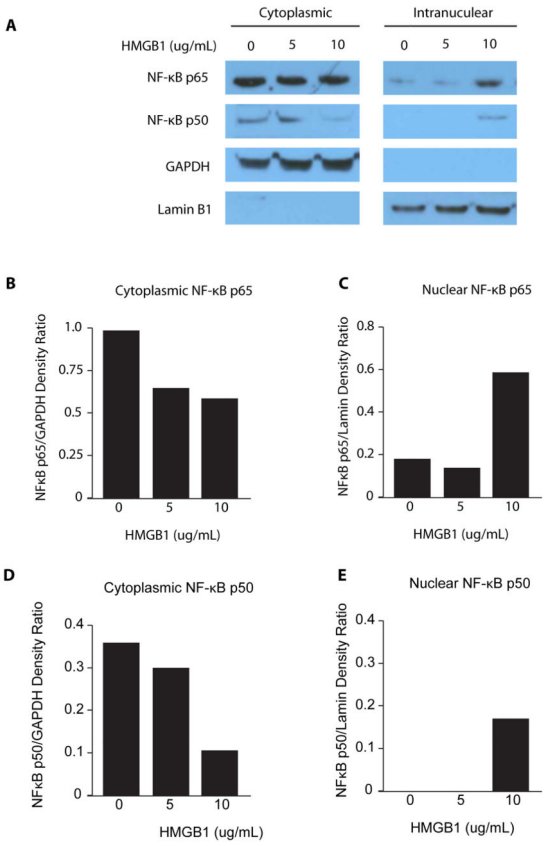

Figure 6.

Representative Western blot of NF-κB activation in rat alveolar type 2 (AT2) cells following exposure to HMGB1. (**A**) NF-κB p65 and p50 translocation from the cytoplasm to the nucleus demonstrated by stimulating AT2 cells with 0, 5, or 10 μg/mL of HMGB1 for 24 hours. (**B–E**) Densitometric analysis was performed using GAPDH as a loading control for the cytoplasmic samples and Lamin B1 as a loading control for the intranuclear samples.

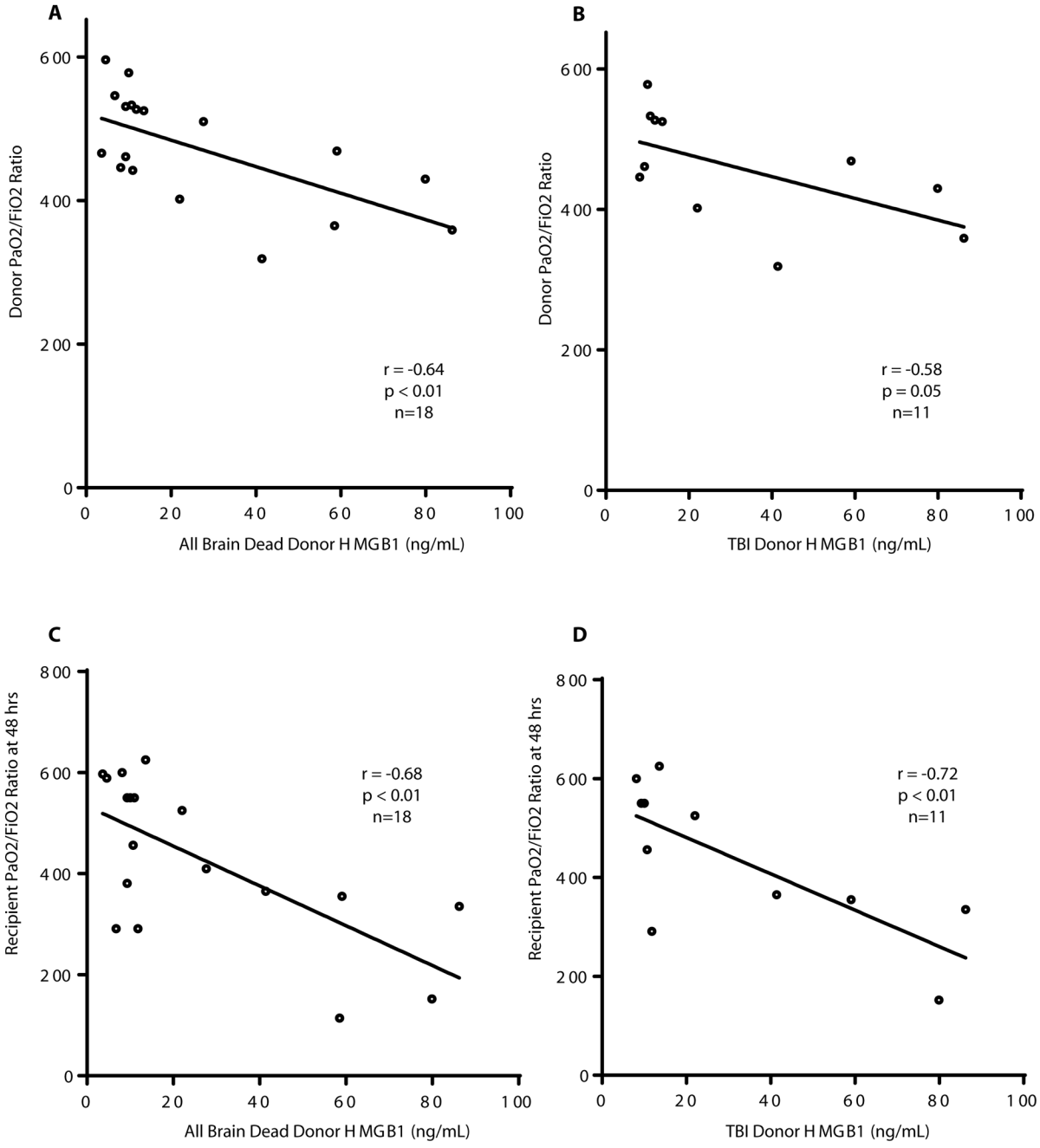

Figure 7.

PaO2/FiO2 ratios in lung transplant donors and recipients based on donor HMGB1 serum concentrations at the time of harvest. (**A**) PaO2/FiO2 ratios among all brain dead donors, regardless of mechanism of injury correlated with donor HMGB1 serum concentrations at harvest. (**B**) PaO2/FiO2 ratios among brain dead donors whose mechanism of injury was TBI, and donor HMGB1 serum concentrations at harvest. (**C**) Recipient PaO2/FiO2 ratios at 48 hours after transplant correlated with donor HMGB1 serum concentrations at harvest. (**D**) Recipient PaO2/FiO2 ratios at 48 hours after transplant from brain dead donors whose

mechanism of injury was TBI correlated with donor HMGB1 serum concentrations at harvest.

Table 1

Donor, Recipient, and Surgery Characteristics (n=18)

Donor Characteristics	
Male sex, n (%)	7 (39)
Age, mean	34.2
Mode of death, n (%)	
Traumatic Brain Injury	11 (61)
Anoxia	4 (22)
Stroke	3 (17)
Race, n (%)	
White	12 (67)
African American	5 (28)
Other	1 (6)
Recipient Characteristics	
Male sex, n (%)	11 (61)
Age, mean	55.3
Pulmonary Diagnosis	
COPD	11 (61)
Idiopathic Pulmonary Fibrosis	5 (28)
Pulmonary Arterial Hypertension	1 (6)
Cystic Fibrosis	1 (6)
Surgery Characteristics	
Transplant type, double, n (%)	18 (100)
Ischemia time in mins, mean	314

18 bilateral lung transplants were performed and donor, recipient, and operative variables were recorded. All donor lungs were donated after brain death.